JOURNAL OF MATERIALS SCIENCE 26 (1991) 3257–3263

Dielectric and microstructural properties of sintered $BaTiO_3$ ceramics prepared from different TiO_2 raw materials

J. F. FERNANDEZ, P. DURAN, C. MOURE
Instituto de Cerámica y Vidrio, C.S.I.C., Electroceramics Department, 28500 Arganda del Rey, Madrid, Spain

$BaTiO_3$ ceramics, sintered from powders previously synthesized using TiO_2 of different characteristics, have been studied. The microstructural development depended on the crystalline nature and impurity types and levels, when the same sintering schedules were applied. Anatase leads to $BaTiO_3$ powders which showed a controlled grain growth after sintering. Rutile with very low impurity levels gave materials in which a non-uniform grain growth was promoted. Dielectric constant and loss tangent were measured and correlated with the density and microstructure. From these correlations, it seems that the raw materials' nature has a greater effect on the dielectric properties that the sintering schedule of a given material.

1. Introduction

Commercial $BaTiO_3$ powders have been traditionally prepared by calcination from oxide or carbonate precursors of Ba and Ti. The reliability and reproducibility of these powders require a rigorous control of the starting raw material characteristics. Powder impurity, morphology, particle size and particle distribution are some of the parameters which must be checked prior to synthesis processing. In previous works [1, 2], it was shown that some local inhomogeneities arise from the incomplete mixing and reacting of the constituents due to the mismatching of sizes of the raw materials. The inhomogeneities give rise to displacements of stoichiometry, from the equimolar compound.

The characteristics of the ceramic powders influenced the microstructure developed in the $BaTiO_3$. Bimodal and non-uniform grain growth must be avoided if enhancement of the dielectric properties is to be attained. The dielectric properties of sintered $BaTiO_3$, in fact, exhibit a strong dependence on grain size [3]. For grain size $< 2\,\mu m$ anomalously high room-temperature permittivity values are obtained together with a general broadening and flattening of the permittivity peak at the Curie temperature. The increase in the dielectric permittivity is possibly caused by both the domain size and the stress effects.

Impurity effects can also significantly affect both the sintering behaviour and the dielectric properties. In a general manner, the presence of impurities can contribute to the liquid-phase formation and to the densification enhancement during the sintering. Their study and control can allow reproducible ceramic microstructures with better dielectric parameters to be obtained. The Ba/Ti ratio is a factor which dramatically influences the microstructural development in $BaTiO_3$. Excess of BaO inhibits grain growth while excess TiO_2 enhances it [4].

In the present work, a correlation between the nature of raw materials and the synthesis and sintering behaviour has been studied. A relationship between microstructure and dielectric properties is proposed.

2. Raw materials

Several TiO_2 with different particle sizes and distributions, aggregation state, crystalline phase and impurity levels have been studied. Their characteristics are summarized in Table I.

TiO_2-anatase have a higher impurity level than the TiO_2-rutile, with P_2O_5 as the most common impurity. TiO_2-anatase powders have a niobium level ranging in the semiconductive zone [5], except for the powder labelled M, but the existence of acceptor cations can compensate the donor effects. TiO_2-M is a modified pigment with alumina and silica. In the case of TiO_2-rutile powders the principal impurity is also P_2O_5; however, the impurity level is lower than in the TiO_2-anatase powders.

The TiO_2-rutile powders have a low agglomerate state; only TiO_2–HPT1 have shown hard aggregates. Having a similar particle size, the specific surface of TiO_2-rutile was lower than that of the TiO_2-anatase.

Two different $BaCO_3$ powders were used. Both have similar impurity levels (0.32%), but different particle size and particle distributions (Table II).

3. Experimental procedure

Equimolar compositions have been prepared from $BaCO_3$-M and all the titanium dioxides. Only TiO_2-M and TiO_2-T were also combined with $BaCO_3$-RPE. $BaTiO_3$ materials were named by an

0022–2461/91 $03.00 + .12

TABLE I Characteristics of TiO_2 raw materials

		$d_{50\%}$ (μm)	Total impurities (%)	Main impurities (⩾ 0.1%)				
				P_2O_5	Nb_2O_5	K_2O	Al_2O_3	SiO_2
TiO_2-anatase								
	M	0.37	0.84	0.38			0.18	0.12
	T	0.37	0.99	0.38	0.35	0.16		
	AT	0.40	0.90	0.23	0.22	0.31		
	ATL	0.40	0.62	0.23	0.22	0.10		
	ATLL	0.43	0.47	0.23	0.22			
TiO_2-Rutile								
	203	1.93	0.07					
	204	0.35	0.33	0.17				
	205	0.36	0.41	0.19		0.14		
	S	1.57	0.04					
	A	1.55	0.02					
	HPT1	3.60[a]	0.09					
	RHP	0.80	0.19	0.12				

[a] Agglomerate size. The particle size 0.1 μm × 0.6 μm.

TABLE II Characteristics of $BaCO_3$

	Impurity (%)				Particle size (μm)
	SrO	CaO	Na_2O	K_2O	
$BaCO_3$–M	0.12	0.07	0.13		2.4
$BaCO_3$–RPE	0.16	0.08	0.01	0.05	4.6

abbreviation of the references of $BaCO_3$ and TiO_2 used; i.e. from $BaCO_3$-M and TiO_2-T we obtained $BaTiO_3$ M–T.

The mixing process was performed by wet zirconia ball milling. The calcining temperature was 1150 °C for all the samples. The $BaTiO_3$ powders were attrition milled with alumina balls. After drying and isostatic pressing into bars at 200 MPa, the samples were sintered in an electric furnace between 1175 and 1450 °C. The crystalline phases were identified by X-ray diffraction (XRD). The microstructure of the sintered ceramic materials was observed by reflection optical microscopy and scanning electron microscopy. Electrical measurements were done using a computerized impedance vectorial analyser (Hewlett Packard 4192A).

4. Results and discussion

4.1. Sintering and microstructure

The synthesis process led to a very pure barium titanate, according to XRD analysis when the $BaCO_3$-M was used with the TiO_2-anatase. Starting from $BaCO_3$-RPE, having large particle size, traces of Ba_2TiO_4 were observed. $BaTiO_3$ synthesized from TiO_2-rutile showed traces of TiO_2-rich secondary phases.

The higher particle growth during the synthesis process corresponded to the finest, most alkaline-rich TiO_2 powders (Table III). The presence of alumina in the TiO_2 does not cause a higher particle growth. In the case of M-203, a reduction of the particle size by milling of the large grains was produced.

Fig. 1 shows the sintering behaviour of the TiO_2-anatase based materials. The highest densities

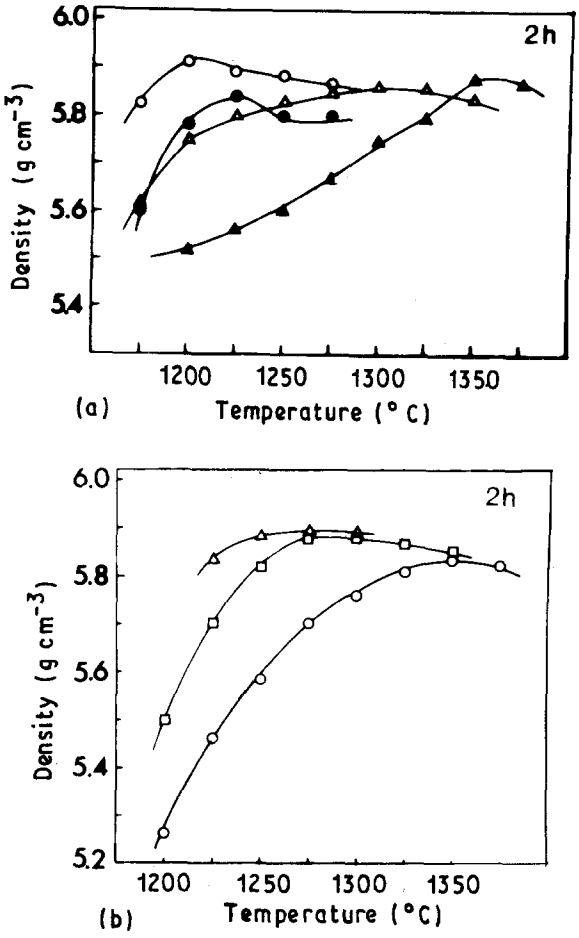

Figure 1 Density versus sintering temperature for the anatase-based $BaTiO_3$. (a) (○) M–M, (△) RPE–M, (●) M–T, (▲) RPE–T; (b) (○) M–AT, (□) M–ATL, (△) M–ATLL.

for the lowest sintering temperature were obtained from the sample M–M. TiO_2-M contains a higher amount of glass forming oxides, SiO_2, Al_2O_3, P_2O_5, etc., than the other titanium dioxides. Small amounts of liquid phase, homogeneously distributed between the equiaxed particles, promote densification at low temperature [1, 6], without exaggerating the grain growth. The microstructure of M–M 1200 °C 2 h (Fig. 2a) corresponds to a highly densified ceramic

TABLE III Grain size distribution for different mixtures (μm)

Granulometry	Sample							
	M–M	M–AT	M–ATL	M–ATLL	M-203	M-204	M-205	M–RHP
$d_{10\%}$	0.52	1.45	1.30	0.58	0.72	0.76	0.76	0.71
$d_{50\%}$	1.05	3.00	2.30	1.10	1.50	1.00	1.05	1.30
$d_{90\%}$	1.75	4.10	3.50	1.60	3.20	1.55	1.95	2.50

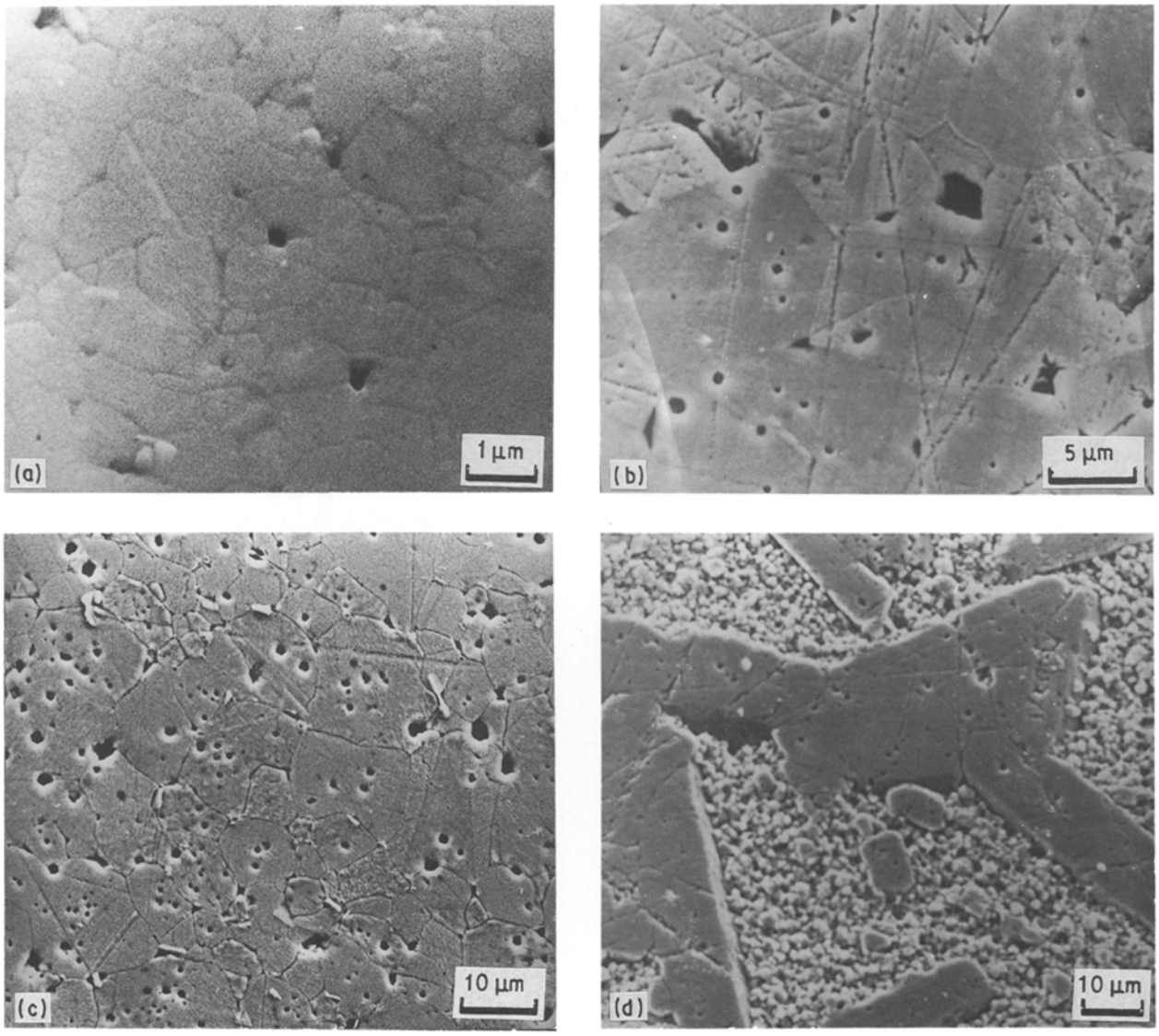

Figure 2 Scanning electron micrographs of (a) M–M 1200 °C 1 h; (b) M–T 1250 °C, 2 h; (c) RPE–M 1325 °C, 2 h, (d) RPE–T 1350 °C, 2 h.

body with little and very localized porosity. No evidence of 90° domain formation was seen for that material. $BaTiO_3$ M–T needed a higher temperature to achieve its maximum density. The existence of niobium in the starting powders favours a charge compensation mechanism which promotes grain growth [7] (Fig. 2b). The charge compensation mechanism took place through titanium vacancies generation [8], which is justified by the existence of $Ba_6Ti_{17}O_{40}$ at the grain boundaries.

In the ceramic materials based on $BaCO_3$–RPE, the inhomogeneities of the starting powders lead to a morphology of $BaTiO_3$ particles with multiple fracture surfaces, which retards the densification process. As a consequence, these materials sintered in a broad temperature range. Several mechanisms were involved in the densification process. In each case the result was a heterogeneous microstructure. In RPE–M the presence of glass forming impurities promotes a rapid growth of grain size in that temperature range (Fig. 2c). A second phase appeared in the surface of the samples after the annealing etching treatment. This second phase does not correlate with the $Ba_6Ti_{17}O_{40}$ compound, as previously reported [9]. EDAX analysis showed little or no presence of Ti cations in these surface compounds. The form and structure of this secondary phase was similar to the compound reported by O'Bryan [10]. The phosphorus comes from

the starting TiO_2 powders, and can be located at the boundaries of the $BaTiO_3$ particles after the synthesis process, like oxides in the system $BaO-P_2O_5-TiO_2$, or like a glass phase in the system $P_2O_5-TiO_2$. In this last case, excess BaO acts as a grain inhibitor. After the decomposition of the glass phase, the nucleation and exsolution of a $Ba_3(PO_4)_2$ phase causes the appearance of a Ti-rich liquid and the corresponding grain growth. Evidence of this hypothesis can be supported by the existence of an abrupt increase in the weight loss during the sintering processes observed in these materials (Fig. 3), at temperatures ranging between 1225 and 1250 °C and above 1300 °C. After this increase in weight loss, an exaggerated grain growth was detected.

On the other hand, the mechanism which involves attainment of maximum density in RPE–T was different, and was attributed to the appearance of a eutectic liquid which promotes exaggerated grain growth (Fig. 2d).

In the M–AT, M–ATL, and M–ATLL series, the higher density values for the low sintering temperatures correspond to $BaTiO_3$ particles which have a lower potassium content.

The densification process of ceramic materials based on TiO_2-rutile was somewhat different (Fig. 4). Two types of behaviour were observed according to the initial impurity levels. For purer materials, the stoichiometric relation was displaced to the TiO_2-rich regions and, as consequence, a rapid densification process in a short temperature range took place. After the initial sintering, which produced the maximum density, a rapid increase in the grain size by means of a TiO_2-rich liquid, causes the decrease in the density values. In some cases, exaggerated grain growth was produced as a consequence of the presence of agglomerates and aggregates which were not broken during milling or compaction processes. The typical microstructure of the more densified sample, based on TiO_2-rutile, is shown in Fig. 5a. The porosity was low and located in the triple points, the grain size was lower than 2 μm, and the fracture was intragranular (Fig. 5b).

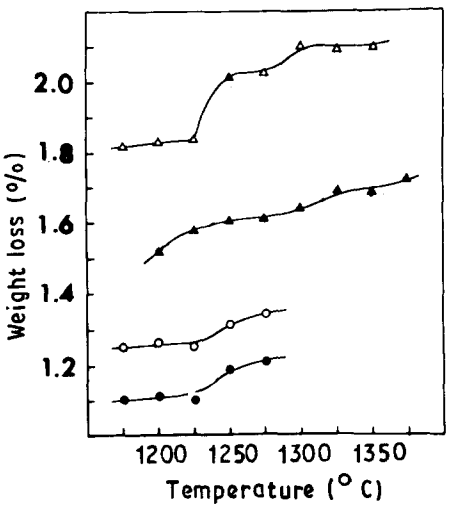

Figure 3 Weight loss during sintering, for 2 h. (△) RPE–M, (▲) RPE–T, (○) M–M, (●) M–T.

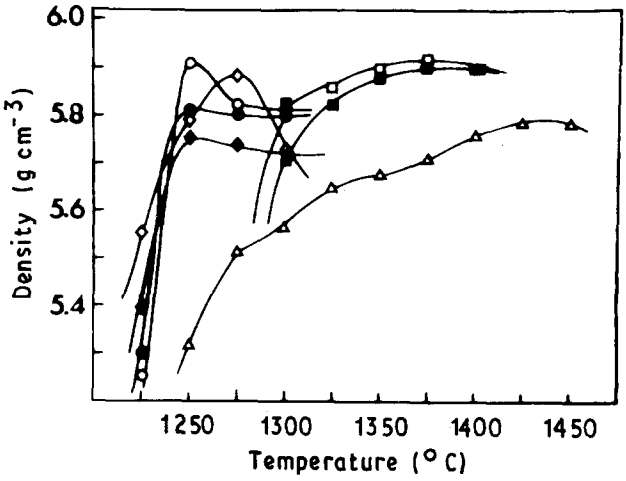

Figure 4 Densification as a function of sintering temperature for the rutile-based $BaTiO_3$, sintered for 2 h. (△) M-203, (□) M-204, (■) M-205, (○) M–A, (●) M–S, (◇) M–HPT1, (◆) M–RHP.

For materials based on TiO_2-rutile with a similar impurity content, a higher temperature was required to obtain maximum densification which runs parallel to a porosity elimination. The grain growth was heterogeneous (Fig. 5c and d), and rapidly progressive above the eutectic temperature. Nevertheless the existence of alumina as an impurity in the raw materials favours in M-205 a higher and more homogeneous grain growth than in M-204. The grains showed straight boundaries which indicated that the driving forces for the sintering processes were minimized. The porosity was principally located on the grain edges as small chains of closed pores, and in the grain interior.

In the cases of M-203, both the particle size and the heterogeneous distribution of the particles retard the densification process up to very high temperatures. Its microstructure showed a grain size of 12 μm (Fig. 5e), and the porosity was of larger size and located at the triple points.

4.2. Microstructure–dielectric properties relationships

Figs 6 and 7 show the values of dielectric parameters plotted against the density of ceramic materials for the different sintering temperatures (temperature increasing in the direction arrowed). In a general view, the dielectric constant diminished when the grain size increased. The dielectric constant was higher for the anatase-based $BaTiO_3$, owing to the small grain size observed in the microstructure. In a first approximation, the existence of an inflection point corresponds to a maximum density value of the ceramic materials. Three different types of behaviour were observed according to these characteristics.

1. Ceramic materials which show a continuous decrease of the dielectric constant with increasing sintering temperature: below the liquid formation temperature the observed microstructures show a high density without grain growth. In this group it is possible to obtain ceramic materials with high dielectric constant ($\varepsilon' \sim 4000$) owing to their small grain size.

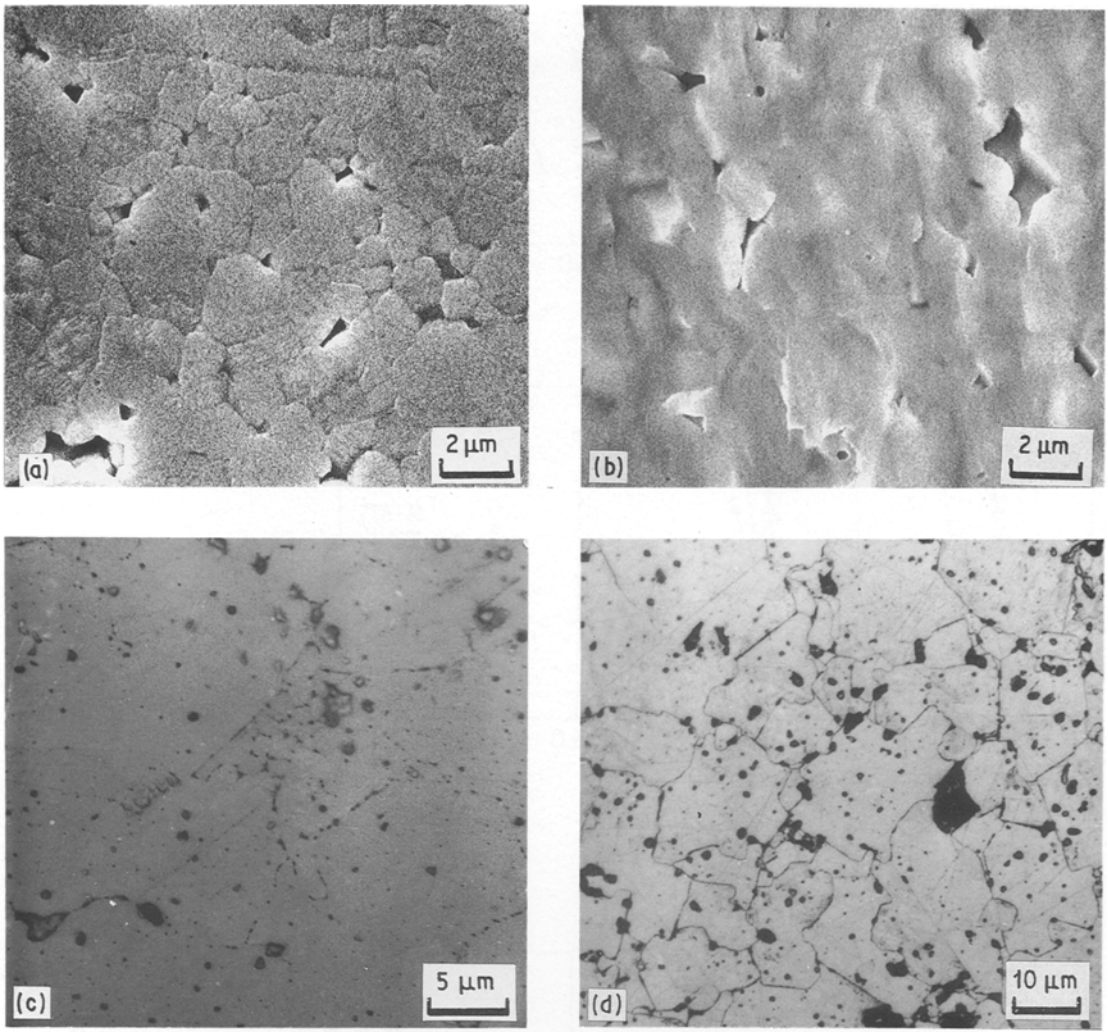

Figure 5 Micrographs of (a) M–HPT1 1275 °C, 2 h, polished and etched surface; (b) M–HPT1 1275 °C, 2 h, fracture surface, (c) M-204 1375 °C, 2 h thermally etched, (d) M-205 1375 °C, 2 h, chemically etched; (e) M-203 1425 °C, 2 h.

2. Ceramic materials which show a maximum value of dielectric constant for the highest densified samples: the materials sintered at temperatures below that corresponding to the maximum density are in an initial sintering stage, without a sintering neck between the particles. Once the maximum density was attained, grain growth occurred, and ε' diminished.

3. Ceramic materials which have a broad sintering temperature range with several maxima in the curve of dielectric constant value maximums: the first maximum can be related to a high density without grain growth, and the second can be associated with increase in conductivity due to the high sintering temperatures, or to the elimination of glass phases, which favours a higher densification.

Tan δ shows a quite different behaviour in comparison to that of ε'. From their variation with density, two groups can be established.

(A) Ceramic materials which show a minimum of tan δ with density and which corresponds approximately to the maximum density value: all the anatase-based $BaTiO_3$ and the M-204 material can be included in this group. The porosity in these ceramic materials was very small. No correlation between tan δ and the location of the porosity was observed. In the case of ceramic material based on anatase, a tendency for the value of tan δ to fall as the grain size increases was observed (Fig. 8). The increase in tan δ in samples densified at a temperature higher than is necessary to attain maximum density, can be related to the evolution of secondary phases (phosphate phases).

(B) Ceramic materials which show a decrease in tan δ with increasing sintering temperature (rutile-based $BaTiO_3$): in these materials an increase in grain size was caused by the presence of a eutectic liquid. The porosity surrounds the grains and diffuses slowly

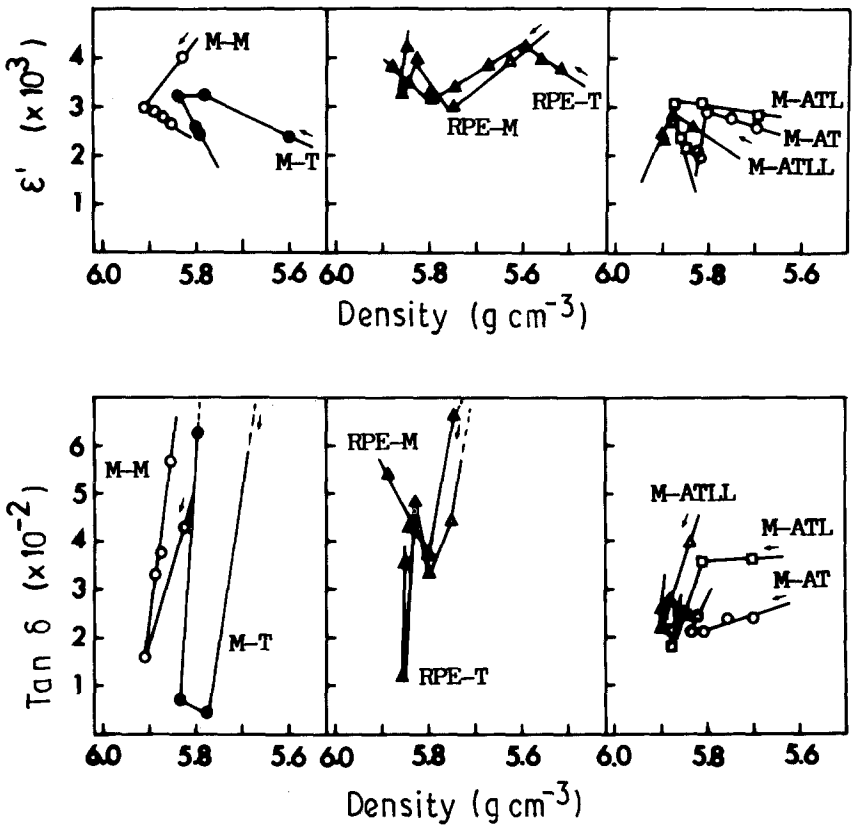

Figure 6 Dielectric parameters versus density of anatase-based $BaTiO_3$. Sintering temperature increases in the direction arrowed.

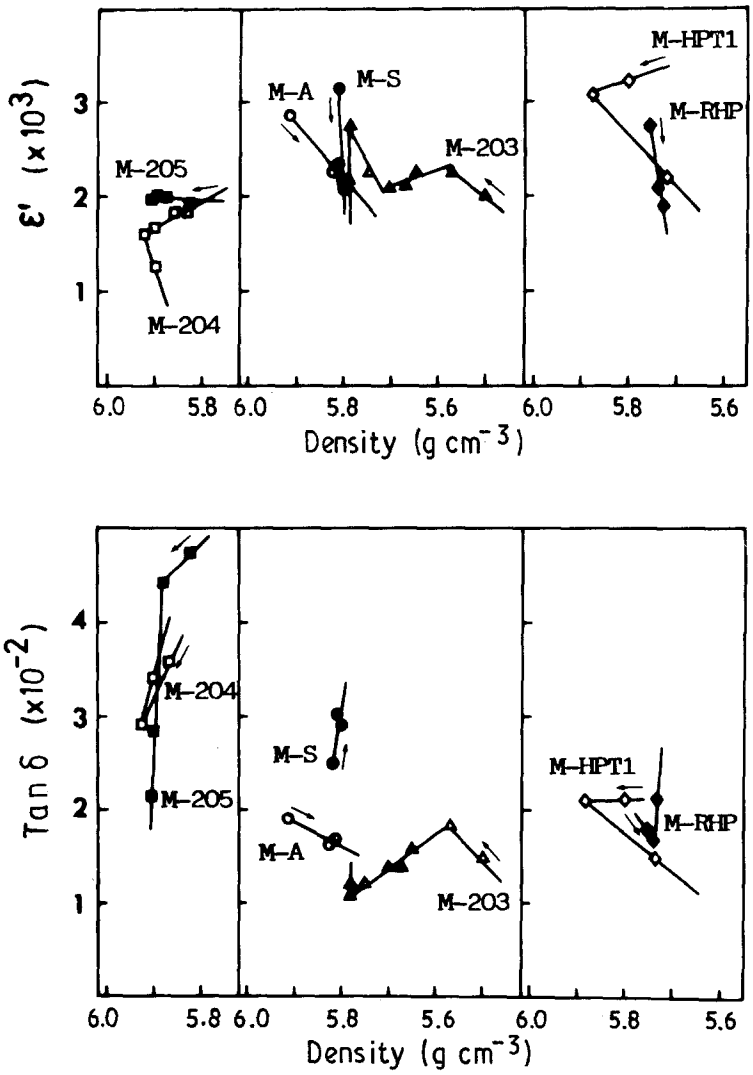

Figure 7 Dielectric parameters versus density of rutile-based $BaTiO_3$. Sintering temperature increases in the direction arrowed.

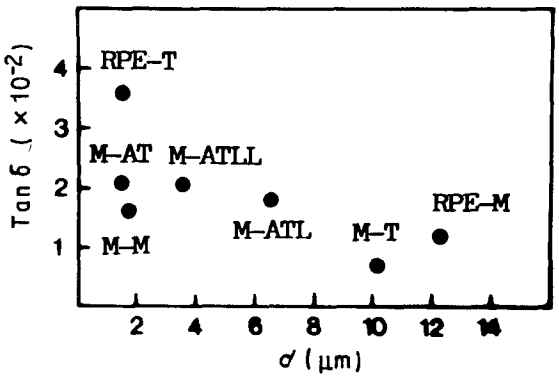

Figure 8 Tan δ as a function of mean grain size for the highest density values of anatase-based $BaTiO_3$.

to the triple points. The elimination of porosity and/or second-phase rich in titanium from the grain boundary could be the reason for the diminishing tan δ with increasing sintering temperature.

From the described results, it is possible to establish a dependence between ε′ and grain size and, on the other hand, between tan δ and second phases and/or porosity. Two aspects are in contradiction with the previously reported relationships [3, 11]: the existence of a high $\varepsilon'(\geqslant 3000)$ in materials with a grain size $> 2\,\mu m$, and the tan δ dependence on grain size.

The influence of porosity was investigated by Okazaki and Igarashi [11]. The porosity affects the dielectric permittivity, decreasing the polarization volume in the volume unit, and increasing the depolarizing field. The depolarization factor is almost proportional to the porosity volumetric fraction, and some deviations were attributed to the porous morphology. The model of cubes [12] introduces the shape factor of the pores, but in this case, no dependence between porosity and tan δ was found. Therefore, closed pores and their location do not influence tan δ. A brick wall model of the microstructure [13] was necessary to understand the influence of the second phases in the polycrystalline materials, which established a dependence between intergranular phases and the grain size of the ceramic materials. For this model, the secondary phase negatively affects tan δ, its influence was stronger for grain size $< 2\,\mu m$, and it depends on the thickness of the secondary phases, due to its high volumetric fraction.

5. Conclusions

The highest dielectric constant values of $BaTiO_3$ were achieved in ceramic materials with a high densification state without grain growth. When exaggerated grain growth was produced from a titanium-rich liquid phase the dielectric constant diminished considerably.

The $BaTiO_3$ ceramic materials can be related to a diphasic system, in which another phase is formed by small quantities of secondary compounds in grain boundaries, promoted by the impurities present in the raw materials, by the remaining titanium-rich liquid phase, and also, by porosity. This secondary phase has a negative influence on the dielectric losses, and for a grain size smaller than 2 μm the influence was stronger, and depended on the thickness of the secondary phase. According to the cubes model, closed porosity and its location do not influence the values of the dielectric losses.

Acknowledgements

The authors are grateful to Rio Rodano S.A. for financial support of this work under contract.

References

1. J. F. FERNANDEZ, P. DURAN and C. MOURE, in "Euro-Ceramic", Vol. 1, "Processing of Ceramics", edited by G. de With, R. A. Terpstra and R. Metselaar (Elsevier, Amsterdam, 1989) p. 1.72.
2. *Idem.*, in "Proceedings of 7th Cimtec Conference, Montecatini", Italy, June 1990.
3. G. ARLT, D. HENNINGS and G. de WITH, *J. Appl. Phys.* **58** (1985) 1619.
4. A. K. MAURICE and R. C. BUCHANAN, *Ferroelectrics* **74** (1987) 61.
5. J. DANIELS and K. H. HÄRDTL, *Philips Res. Report* **31** (1976) 487.
6. M. F. YAN, in "Advances in Ceramics", Vol. 21, "Ceramics Powder Science" (The American Ceramic Society, OH, 1987) p. 635.
7. G. M. DYNNA and Y. M. CHIANG, in "Ceramic Transactions", Vol. 7, "Sintering of Advanced Ceramics" edited by C. A. Handwerker, J. E. Blendell and W. Kaysser (The American Ceramic Society, OH, 1990) p. 547.
8. H. M. CHAN, M. P. HARMER and D. M. SMITH, *J Amer. Ceram. Soc.* **69** (1986) 507.
9. M. DROFENIK, S. PEJOVNIK, L. IRMANCNIK, I. MOCNIK and V. K. DRASEVEC, *Mater. Sci. Monogr.* **14** (1982) 361.
10. H. M. O'BRYAN Jr, *Amer. Ceram. Soc. Bull.* **66** (1987) 677.
11. K. OKAZAKI and H. IGARASHI, in "Ceramic Microstructure '76", edited by R. M. Fulrath and J. A. Pask (Westview Press, Boulder, Colorado, 1976) p. 564.
12. H. BANNO, *Amer. Ceram. Soc. Bull.* **66** (1987) 1332.
13. D. A. PAYNE and L. E. CROSS, in "Microstructure and Properties of Ceramic Materials", Proceedings of the First USA-China Seminar, edited by T. S. Yen and J. A. Pask (Science Press, Beijing, China, 1984) p. 380.

Received 13 June
and accepted 26 June 1990